and $\sigma_R \equiv 128$ MPa for the tempered glass used here, Eq. (A-3) gives $P_c(\sigma_R) \approx 2P_c(0)$.

Acknowledgment: The writers thank G. Garrett for assistance in collecting the data.

References

[1] S. M. Wiederhorn and B. R. Lawn, "Strength Degradation of Glass Impacted with Sharp Particles: I"; this issue, pp. 66–70.
[2] F. M. Ernsberger, "Strength of Brittle Ceramic Materials," *Am. Ceram. Soc. Bull.*, **52** [3] 240–46 (1973).
[3] D. B. Marshall and B. R. Lawn, "Strength Degradation of Thermally Tempered Glass Plates," *J. Am. Ceram. Soc.*, **61** [1–2] 21–27 (1978).
[4] D. B. Marshall and B. R. Lawn, "Measurement of Nonuniform Distribution of Residual Stresses in Tempered Glass Discs," *Glass Technol.*, **19** [3] 57–58 (1978).
[5] D. B. Marshall and B. R. Lawn, "An Indentation Technique for Measuring Stresses in Tempered Glass Surfaces," *J. Am. Ceram. Soc.*, **60** [1–2] 86–87 (1977).
[6] B. R. Lawn and A. G. Evans, "A Model for Crack Initiation in Elastic/Plastic Indentation Fields," *J. Mater. Sci.*, **12** [11] 2195–99 (1977).
[7] B. R. Lawn and M. V. Swain, "Microfracture Beneath Point Indentations in Brittle Solids" *ibid.*, **10** [1] 113–22 (1975).
[8] S. M. Wiederhorn and D. E. Roberts, "A Technique to Investigate High Temperature Erosion of Refractories," *Am. Ceram. Soc. Bull.*, **55** [2] 185–89 (1976).
[9] B. R. Lawn and D. B. Marshall, "Contact Fracture Resistance of Physically and Chemically Tempered Glass Plates: A Theoretical Model," *Phys. Chem. Glasses*, **18** [1] 7–18 (1977).
[10] A. G. Evans and T. R. Wilshaw, "Quasi-Plastic Solid Particle Damage in Brittle Materials: I," *Acta Metall.*, **24**, 939–56 (1976).
[11] B. R. Lawn and D. B. Marshall; pp. 205–29 in Fracture Mechanics of Ceramics, Vol. 3. Edited by R. C. Bradt, D. P. H. Hasselman, and F. F. Lange. Plenum, New York, 1978.
[12] R. Hill, Mathematical Theory of Plasticity; p. 97. Clarendon, Oxford, England, 1950.

Quenched Metastable Glassy and Crystalline Phases in the System Lithium-Sodium-Potassium Metatantalate

KURT NASSAU, CHRISTINE A. WANG, and MICHAEL GRASSO

Bell Laboratories, Murray Hill, New Jersey 07974

A twin-roller apparatus was used to quench 21 melts in the three pseudobinary systems and in the pseudoternary system composed of $LiTaO_3$, $NaTaO_3$, and $KTaO_3$. Glasses were obtained in all but the high-Na region. X-ray diffraction and differential thermal analysis studies of the metastable compositions showed that there were two metastable crystalline phases when the materials crystallized; one phase was a defect pyrochlore structure centered at $KTaO_3$ and the other appeared at $Li_{0.8}K_{0.2}TaO_3$. The metastable phases subsequently transformed into the expected stable phases on heating. There is some evidence for a subsolidus two-glass region in the system (K,Na)TaO_3.

I. Introduction

QUENCHED oxide glasses composed solely of non-glass-forming components (i.e. not containing SiO_2, B_2O_3, P_2O_5, etc.) can show interesting pyroelectric- and ferroelectriclike dielectric properties.[1] The presence of a dc component in the dielectric loss led to the observation of large ionic conductivities of $\approx 10^{-6}$ Ω·cm in $LiNbO_3$and $LiTaO_3$.[2] This observation prompted a systematic examination of the occurrence of vitreous phases and phase transitions in systems containing Li, Na, and K tantalates and the equivalent niobate and mixed niobate-tantalate systems.[3] Dielectric and related properties are reported elsewhere.[4]

The quenching of metallic glasses is a widely studied field with reviews[5,6] and a bibliography[7] but much less work has been done in the field of non-glass-forming compound oxides. Surveys by Sarjeant and Roy[8] and Suzuki and Anthony[9] and limited systematic studies for the mixed lanthanide oxides[10] and lanthanide oxide-alumina systems[11] are available. Kokubo *et al.*[12] examined the system mixed alkali-Ta_2O_5-Nb_2O_5-Al_2O_3 for glass formation, using rather low quenching rates which resulted in glass formation only in the presence of Al_2O_3. They also examined[13,14] some quenched compositions in the system K_2O-Ta_2O-Nb_2O_5-Al_2O_3-SiO_2 and found a metastable pyrochlore phase; glass was reported only in compositions containing SiO_2 or Al_2O_3. Sarjeant and Roy[15] reported extended glass formation in the system Na_2O-Ta_2O_5 and K_2O-Ta_2O_5 but gave no further details. Gossink[16] summarized the work on glass formation in the alkali tungstate and molybdate systems.

Received March 30, 1978; revised copy received June 15, 1978.

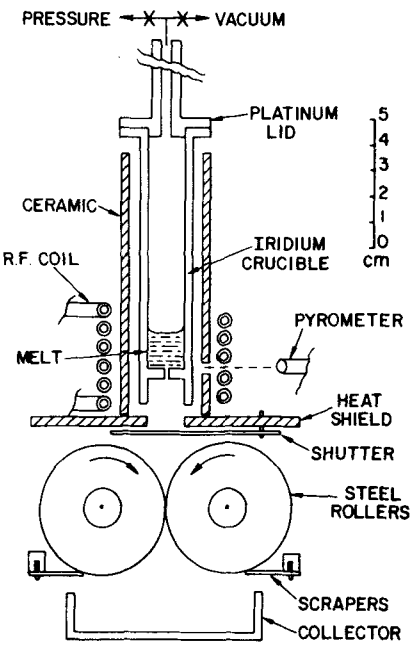

Fig. 1. Apparatus used for the quenching of oxide melts.

II. Experimental Procedure

Samples were prepared from reagent-grade oxides and carbonates by multiple grinding, ball-milling, and sintering for several days, usually to a maximum of 1000°C. Initially, samples were prepared at 20 mol% intervals in the binary systems and at the 1/3 ratio points in the ternary, with intermediate compositions as needed.

Samples were quenched in the twin-roller apparatus of Chen and Miller,[17] modified to permit operation with oxides melted in a crucible (Fig. 1). Samples weighing ≈5 g and ground to pass through a 125-μm screen were melted in an iridium crucible (110 mm long, 16 mm ID, and 1.5 mm wall thickness with an orifice 0.025 to 0.04 mm in diam.). A 5 mm extension beyond the end of the tube ensured uniformity of the temperature. Power was applied

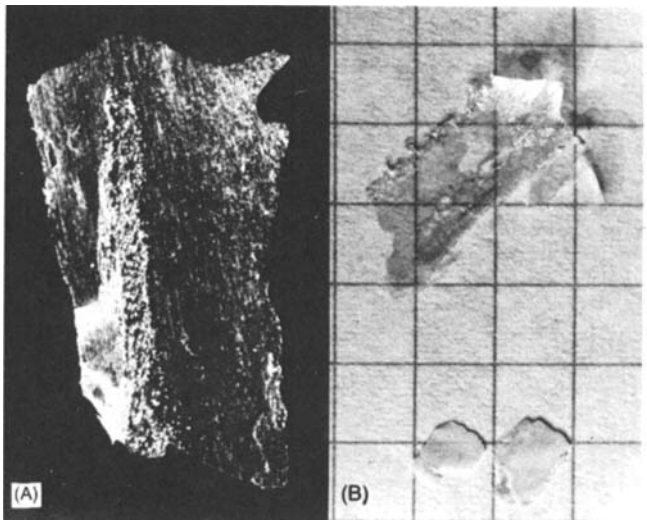

Fig. 2. Flakes of quenched tantalates. (*A*) Flake of $Li_{0.3}K_{0.7}TaO_3$ (8 mm long) showing glassy and crystalline areas; surface detail originates from scoring on rollers. (*B*) Glassy (top) and heated crystallized flakes of $K_{0.6}Na_{0.4}TaO_3$; edge of square is 5 mm long.

by a 5-turn coil fed from a 4.5 kHz 25 kW radio frequency generator.*

Suction of ≈0.01 atm was used during the melting stage to prevent premature leakage (not required in operation with alloys, which do not wet the fused silica containers). The temperature was read on an uncorrected optical pyrometer sighted on the crucible wall (Fig. 1). Quenching resulted when the molten contents were squirted out of the crucible with a pressure of ≈1.5 atm and injected between the 5-cm-diam. chrome-plated steel rollers rotating at 3000 rpm. The quenching rate is estimated as $\approx 10^7$ degrees/s.[3]

Differential thermal analysis (DTA) was conducted in Pt cups in the high-temperature cell of a thermoanalyzer† in flowing N_2. Preliminary data indicated no significant variation in the results for heatings of 5°/min to 50°/min, and all subsequent work was done at 20°/min; this relatively high rate gave clear indication of broad, time-dependent transitions (which may be lost at low heating rates) and also permitted rapid analysis. Transition temperatures were recorded as the extrapolated onset of each peak. In view of the relatively broad nature of even the sharpest of the transitions observed, it was felt that rounding off temperatures to the nearest 10° was appropriate. Grinding the flakes had no significant effect on the DTA pattern.

X-ray diffraction (XRD) was performed on a diffractometer‡ with Ni-filtered Cu radiation at 30 kV peak and 10 mA. Survey patterns were taken at 2°/min. Samples were usually ground and applied to a microscope slide with an acetone-collodion adhesive. Some quenched flakes of each composition were also examined without grinding by supporting them in the X-ray beam on a pair of thin glass fibers with a trace of oil as adhesive. Precision data were recorded with a Guinier camera§ using Cu radiation; line positions were corrected by using α-Al_2O_3 as an internal standard. The indexing of new phases was attempted by a combination of the manual Ito's technique and the computerized version of Visser.[18]

Some quenched flakes were examined on a scanning electron microscope¶ operated at 20 kV and equipped with an X-ray energy spectrometer.‖ Some compositions were checked using single crystals as standards. Ferroelectric Curie temperatures[4] provided a second check on stoichiometry, which was found to be satisfactory.

III. Results

Roller-quenching appeared to give optimum results when the melt was ≈100° to 250°C above the melting point. The resulting glass flakes were ≈10 μm thick and up to 5 by 10 mm in area and were very brittle. They were nearly colorless; sometimes the central area was transparent and glasslike with opaque, polycrystalline edges, or vice versa. Figure 2 shows some flakes; the surface texture derives from scraper-produced scoring on the rollers. A diffraction pattern of two or three selected flakes was checked, with absence of diffraction lines taken as a probable indication of glass formation. Frequently, ground flakes showed somewhat more crystallinity than the flakes themselves, either because they contained more crystalline regions (being less carefully selected) or because grinding might have produced some additional (but never complete) crystallization.

Results of DTA on ground flakes were next examined. An exotherm, particularly if preceded by a glass transition at a temperature T_g, was taken as confirmation of the existence of a vitreous phase *G* (for glass). The designations *E*, *E'*, *L*, and *J* were used for stable and *M* and *N* for metastable crystalline phases.

The quenching temperatures in Table I gave near optimum

*Lepel High Frequency Laboratories, Maspeth, N.Y.
†Model 990, E. I. du Pont de Nemours & Co., Inc., Wilmington, Del.
‡Miniflex, Rigaku Corp., Chiyoda-ku, Tokyo, Japan.
§XDC700, Irdab, Stockholm, Sweden.
¶Autoscan, Etec Corp., Hayward, Calif.
‖5100C, Kevex Corp., Burlingame, Calif.

Table I. Tantalate Compositions Quenched and Thermal Transformations

Composition (mol%)			Quench conditions		
$LiTaO_3$	$NaTaO_3$	$KTaO_3$	Temp.† (°C)	No.	Thermal transition sequence‡
100			1850	7	*JG* 570–630 *J*
	100		1850–1950	4	Crystal only
		100	1450	3	*G*{*M*} 520* 600 *M* 670 *ME-E*(*M*) 890 *E*
80	20		1700	9	*JG* 600–630 *J*(*E*)
60	40		1700–2000	6	Crystal only
40	60		1800–1850	2	Crystal only
20	80		1750–1790	2	Crystal only
	80	20	1900–2000	2	Crystal only
	60	40	1950	4	*G* 530-590 *E'* 620 *E'M* 710–800 *E*
	40	60	1750	2	*G* 620 *M*(*E'*) 720–790 *E*
	20	80	1550	4	*G* 590* 630 *M*(*E'*) 700–850 *E*
20		80	1475	1	*MG* 560 *M*(*L*) 600 *M*(*EL*) 680–750 *EL*
40		60	1550	1	*G* {*L*} 600 *L*
60		40	1550	1	*G* 600 *L* 630 *LJ*
70		30	1700	1	*LG* 600 *L* 640 *LN* 680 *LJ*
80		20	1625	1	*G* 660 *N*(*LJ*) 730 *JL*
90		10	1600	1	*GJ* 630 *JN*(*L*) 670 *J*(*L*)
33.3	33.3	33.3	1620	1	*G* (*E*) 580 *EL*
60	20	20	1620	1	*G*{*J*} 600–630 *EL*(*N*) 670 *JLE*
20	60	20	1750–1975	5	Crystal only
20	20	60	1650	2	*G*{*M*} 580 *ELM* 660–760 *EL*

†Quench temp. for best *G* is given; if crystal only, full range tried is given. ‡Symbols given in estimated order of amount present; ( ) indicates small amount, { } indicates partial X-ray pattern only. Transitions are exotherms except for glass transitions marked *; major peaks underlined; temperatures in °C.

results, although sometimes considerable variation made little difference, as in the seven $LiTaO_3$ quenches at 1700° to 1890°C. However, if glass could not be obtained, the full range of quenching temperatures tried is given, e.g. the six attempts for $Li_{0.6}Na_{0.4}TaO_3$ at 1700° to 2000°C.

Typical DTA curves are shown in Fig. 3. There was often more than one exotherm (e.g. the $Li_{0.8}K_{0.2}TaO_3$ shown) in which case a specimen was X-rayed after removal from the DTA apparatus after each peak (Fig. 4(*A*)). If broad peaks occurred (as in the $KTaO_3$ of Fig. 3) the temperature range is given as full peak range less the inherent machine/sample width of a sharp transition peak (a net range of 670° to 890°C for $KTaO_3$). Additional samples were taken from near the center of such broad peaks and helped to clarify the nature of the slow transition involved, in this instance the *M* to *E* transition (Fig. 4(*B*)).

No thermal effects were seen during cooling and reheating after each exotherm (at least not until after passing the original exotherm temperature), indicating that each of the exotherms represented an irreversible transition. The results obtained are summarized in Fig. 5.

IV. Discussion

(1) The Occurrence of Glass

The most difficult decision in examining rapidly quenched materials is whether the designation "glass" should be used. Certainly there can be no disagreement with the designation amorphous or with NCS (noncrystalline solid) or SROO (short range order only) solid as discussed by Roy.[19] The material is transparent, shows no crystallinity under X rays (at most a broad diffuse scattering of several degrees to >10° in width as in Fig. 4(*A*)) or under electron microscopy, shows a glass transition at some compositions, shows a mixed-alkali effect in the variation of conductivity with concentration[4(b)] (just as conventional glasses do[20]), and crystallizes exothermically over a narrow temperature region. In designating such a material as *G*, we believe that these are true glasses in the sense of being metastable quenched liquids and not merely crystalline materials which are so finely divided as to appear amorphous.

Glass was observed in the whole system $Li_xK_{1-x}TaO_3$, in the system $K_xNa_{1-x}TaO_3$ up to $x=0.6$, and in the system $Na_xLi_{1-x}TaO_3$ at $x>0.8$ (Fig. 5 and Table I). At some of these

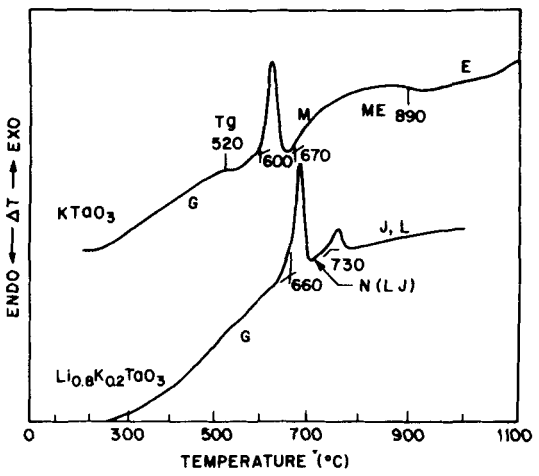

Fig. 3. Typical DTA curves taken at 20°/min in flowing N_2.

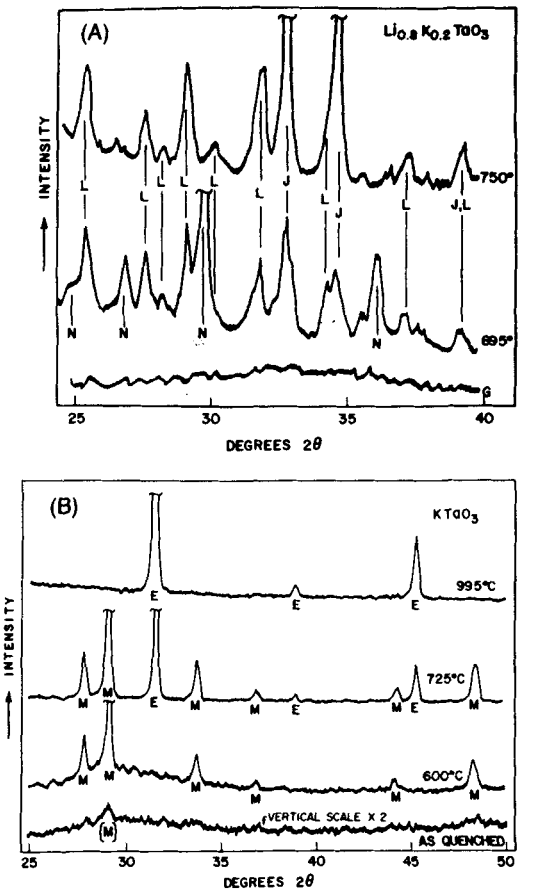

Fig. 4. Powder X-ray diffraction patterns for (*A*) $Li_{0.8}K_{0.2}TaO_3$ and (*B*) $KTaO_3$.

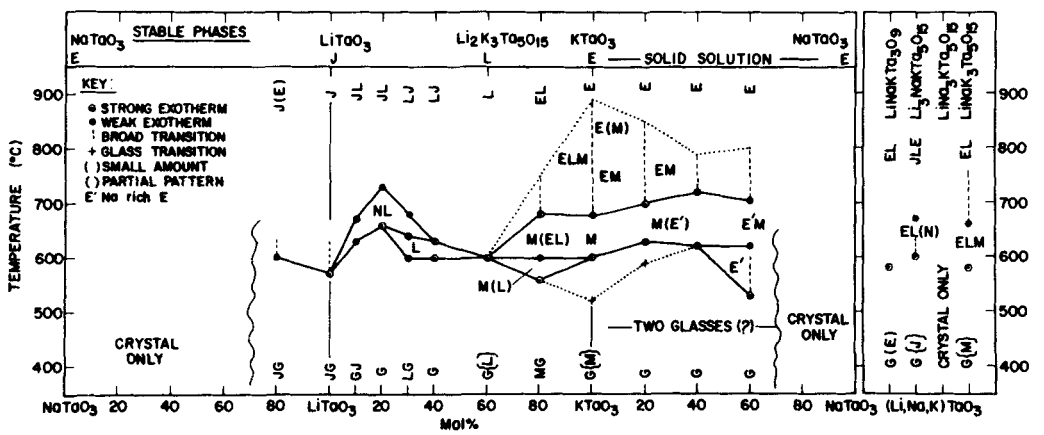

Fig. 5. Phase transformation diagrams for quenched glasses in the (Li,Na,K)TaO_3 system.

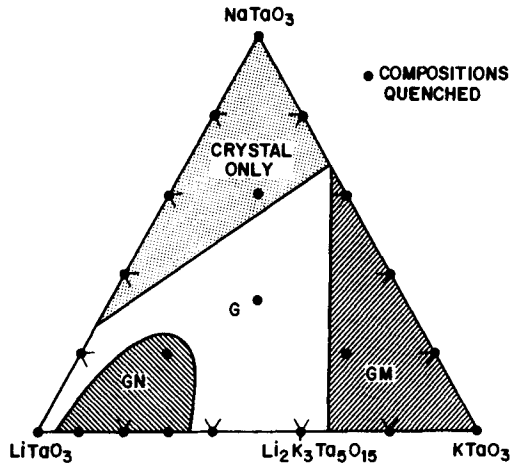

Fig. 6. Occurrence of metastable phases in the (Li,Na,K)TaO_3 system.

Table II. X-Ray Data for Structure *M

hkl	d_{calc} (Å)	d_{obs} (Å)	I_{obs}
100	10·590	10·9†	vw
111	6·114	6·116	vs
311	3·193	3·192	ms
222	3·057	3·058	vvs
400	2·6475	2·648	s
331	2·4295	2·429	vw
511,333	2·0380	2·038	w
440	1·8721	1·872	ms
531	1·7900	1·790	m
622	1·5965	1·596	m
444	1·5285	1·529	m
551,711	1·4829,	1·482	m
731,553	1·3787	1·378	w
662	1·2148	1·214	w
840	1·1840	1·184	vvw

*Metastable $KTaO_3$ at 660 C; cubic, a = 10.590 A. V = 1187.6 A.^{3} †Uncorrected from diffractometer trace only; all other d_{obs} values corrected from Guinier data.

compositions significant quantities of crystalline material were present with the glass. Glass transitions were observed only in $KTaO_3$ and $K_{0.8}Na_{0.2}TaO_3$, in contrast to the niobate systems where glass transitions predominate.[3]

It is interesting to contrast this system, where only Na-rich compositions do not form glasses (as well as the niobates,[3] where the same is true) with the alkali molybdates and tungstates.[16] In the case of the molybdates (and particularly the $M_2Mo_2O_7$ compositions), Li forms glass most easily, with increasing difficulty as the ionic radius increases through Cs. The same is true for the $M_2W_2O_7$ compositions, except that here Na is the best glass former and Li has an anomalous position between Rb and Cs. The difference may lie in the different crystal structures, formation energies, and hence ease of crystallization of the stable crystalline phases involved. Note that critical cooling rates to prevent crystallization in the tungstates and molybdates ranged down to as little as the 1°/s for $NaKMoWO_7$.

(2) Stable Crystalline Phases

For every composition tested, the final phase assemblage before melting occurred was that expected from equilibrium among the stable phases shown at the top of Fig. 5. In all cases the X-ray powder patterns were consistent with those available in the JCPDS X-ray diffraction file.[21] Since essentially all of these stable phases and phase diagrams involve ferroelectricity, detailed summaries and the many references may be found compiled in Landolt-Boernstein.[22] These data may be summarized as:

(1) The perovskite structure occurs for $NaTaO_3$ (JCPDS No. 25–863), $KTaO_3$ (JCPDS No. 2–822), and for solid solutions between them. The $NaTaO_3$ transforms from orthorhombic to tetragonal to cubic as temperature increases, but the distortions from the cubic $KTaO_3$ perovskite structure are relatively small. The powder patterns show such reductions of symmetry as splitting of the lines but these changes were not investigated in the present study and all phases in this group were treated as (pseudo-)cubic and designated E. There is, however, a significant change in the cubic lattice parameter between the two end members from 3.99 for $KTaO_3$ to 3.89 Å for $NaTaO_3$[23,24] and, if a phase on initial crystallization did not have the lattice parameter corresponding to its equilibrium composition E at higher temperatures, the designation E' was used to indicate the presence of an Na-rich crystalline phase.

(2) The $LiTaO_3$ (JCPDS No. 9–187) (J) and the tungsten bronze structure $Li_2K_3Ta_5O_{15}$ (JCPDS No. 23–1198) (L) are the only other stable crystalline phases reported in the (Li,Na,K)TaO_3 system. No others were observed in the present work.

These designations, together with G, M, and N, indicate phases in the three pseudobinary phase diagrams of Fig. 5. The pseudoternary (Fig. 6) shows the range of occurrence of the three metastable phases G, M, and N; this figure corresponds to the "quenched phase plot" of Giessen.[25] These diagrams are based on the DTA and XRD data of Table I.

(3) Metastable Crystalline Phases

(A) Phase M: This metastable phase was observed at $Li_{0.2}K_{0.8}TaO_3$ to $KTaO_3$ to $K_{0.4}Na_{0.6}TaO_3$ and also at $Li_{0.2}Na_{0.2}K_{0.6}TaO_3$. The indications are that the M-phase composition is fixed at $KTaO_3$ (with the possibility of some minor solid solution incorporation of Li and/or Na) and accordingly is a polymorph of the perovskite phase. In $KTaO_3$ the M phase forms from the glass at 600°C and begins to decompose to the stable $KTaO_3$ perovskite structure at 670°C by a time- and temperature-dependent process as previously described (Section III).

Table II gives the observed d spacings and an indexing based on cubic symmetry with $a = 10.590$ Å. This indexing gives a unit cell volume of 1187.6 Å^3 and a calculated density of $D = 0.375Z$, where Z is the number of molecules per unit cell. A plausible $Z = 16$ for a pyrochlore structure gives a $D = 6.00$ g/cm^3, somewhat less than the 7.02 g/cm^3 of stable $KTaO_3$, as expected for a metastable phase.

This phase appears to be the same as that reported by Kokubo *et al.*[13,14] in the composition they designated as $K_{1.5}(Ta_{0.65}Nb_{0.35})_2O_{5.75}$. This composition was obtained by rapid cooling of a melt of batch composition 40.0 mol% $KO_{0.5}$, 26.0 $TaO_{2.5}$, 14.0 $NbO_{2.5}$, 13.3 $AlO_{1.5}$, and 6.7 SiO_2; the analyzed mol% composition was 32.2, 29.3, 15.7, 15.1, and 7.6, respectively. This composition quenched to a glass and, when heated, crystallized to a metastable phase which finally yielded the expected perovskite. When the metastable composition was leached with hot 2N HCl, followed by cold 2N NaOH, a powder remained with the analyzed composition 26.3 mol% $KO_{0.5}$, 45.2 $TaO_{2.5}$, 22.6 $NbO_{2.5}$, 2.5 $AlO_{1.5}$, and 3.4 SiO_2. This powder was indexed on the cubic defect pyrochlore structure with $a = 10.62$ Å as $K_{2-2\delta}(Ta_{0.65}Nb_{0.35})_2O_{6-\delta}$. By calculating diffraction intensities to match the observed powder pattern, the formula $K_{1.5}(Ta_{0.65}Nb_{0.35})_2O_{5.75}$ was deduced, completely ignoring the Al and Si content.

The pyrochlores[26] (also known as the atopites[27]) are a large group of substances with the general formula $M_2^{II}M_2^{V}O_7$ or $M_2^{III}M_2^{IV}O_7$. Much substitution occurs, and one of the oxygens may be missing with appropriate changes in the metals for charge neutrality in the defect pyrochlores. There are eight molecules in the unit cell with only one variable parameter; the lower valence metal is in a cubic site (normal to distorted) and the higher valence metal is in an octahedral site (deformed to regular), respectively. There may also be a tetragonal distortion.

Application to the $KTaO_3$ M phase gives the relation to the pyrochlore $Ca_2Ta_2O_7$ by omitting one CaO to obtain $CaTa_2O_6$ and then replacing Ca^{2+} by $2K^+$ to give $K_2Ta_2O_6$ or $KTaO_3$ as a defect pyrochlore. The present data cannot distinguish between $KTaO_3$ and $K_{1-2\delta}TaO_{3-\delta}$; however there is no need for such a further defect formulation at present. The formulation of Kokubo *et al.*[13,14] cannot be accepted uncritically since they completely ignored the Al and Si content; the difference between their nominal batch and analyzed glass compositions indicates that some uncertainty exists, and it is

Table III. X-Ray Data for Structure *N

d_{obs}(Å)†	I_{obs}
4.67	vvvw
4.16	s
3.75	vs
3.56	vvw
3.296	vw
2.984	ms
2.482	m
2.287	vw
2.082	w
1.832	vw

*Metastable $Li_{0.8}K_{0.2}TaO_3$ at 700°C. †From corrected Guinier data.

quite possible that the leaching used may have affected the composition.

The powder pattern of Table II gives an excellent fit with $a = 10.590$ Å, which is in reasonable agreement with the limited set of intensities given by Kokubo *et al.*,[13] who do not give d spacings but give $a = 10.62$ for the mixed potassium niobate tantalate.

(B) Phase N: This new metastable phase was observed from $Li_{0.9}K_{0.1}TaO_3$ to $Li_{0.7}K_{0.3}TaO_3$ and also at $Li_{0.6}Na_{0.2}K_{0.2}TaO_3$. The $Li_{0.8}K_{0.2}TaO_3$ composition was examined in some detail; here the *N* phase forms from the glass at 660° and converts to the stable assemblage of $J+L$ at 730°C. A listing of d spacings is given in Table III; indexing attempts were unsuccessful.

(4) Phase Transformations

A diagram like Fig. 5 is best termed a metastable phase transformation diagram to indicate its limitations. It is quite different from the metastable phase diagram of the metals field,[5] which shows the nature of the phases produced by different supercooling temperatures. The phase rule does not apply to any such metastable diagrams, except to the final high-temperature equilibrium-phase assemblages. Ostwald's step rule may be expected to apply to a metastable transformation diagram in the sense that when a metastable state "is spontaneously destroyed, the solid phase produced is not the most stable under the existing conditions, but the next in order."[28] Certainly the system will continue to reduce its free energy as it goes through successive phase transformations. The choice of alternative possible transformation paths is probably kinetically controlled, i.e. the phase to nucleate first would take over completely, whereas in the case of multiple nucleation the phases can coexist, with the phase having the higher subsequent growth rate becoming dominant. Additional complications can derive from a metastable subsolidus solubility gap, resulting in phase separation, possibly indicative of a two-glass region. In such instances, diffusion becomes involved in the transformations. There are surprisingly few general principles which could limit the possible phenomena in such a phase-transformation diagram. Metastable phase diagrams in conventional glass-forming systems were discussed by Steward[29] and for the metallic glasses by Giessen and Willens.[5] A general classification of transitions was given by Roy.[30]

In the system $Na_xLi_{1-x}TaO_3$, glass was obtained only for $x = 0.2$ and 0.0. In both instances the crystallization occurred directly to the stable phase assemblage with moderately slow transformations in the 30° and 60° range.

From $Li_{0.9}K_{0.1}TaO_3$ to $Li_{0.7}K_{0.3}TaO_3$ the new metastable phase *N* appears over a narrow temperature region. From $Li_{0.9}K_{0.1}TaO_3$ to $Li_{0.6}K_{0.4}TaO_3$, this new phase or a combination of *N* and *L* is the first to crystallize; *J* appears only after an additional exotherm. At $Li_{0.7}K_{0.3}TaO_3$ there are three exotherms with the transformations *G* to *L* at 600°, *G* to *N* at 640°, and *N* to *J* or *N* to $J+L$ at 680°C, resolved on the basis of DTA and X-ray results. In this region there are only sharp exotherms, indicating rapid transformations.

Over the region $Li_{0.2}K_{0.8}TaO_3$ to $KTaO_3$ to $K_{0.4}Na_{0.6}TaO_3$ the *M* phase appears; it can be deduced that this phase is a polymorph of $KTaO_3$. Two distinct slow transformations can be recognized in this region. In pure $KTaO_3$ the pure *M* phase transforms to pure *E* over the rather broad range of 670° to 890°C. As the sample temperature was increased at the 20°/min heating rate, the conversion from *M* to *E* proceeded gradually with 52% *M* remaining at 725°, 33% at 830°, and 0% at 995°C, as judged from the relative intensities of the diffraction peaks. This effect is not a pure temperature one, since the reaction proceeded by holding at 750°C, decreasing from 52% *M* to 31% after 2 h, and to 19% after 18 h. This behavior may be due to a diffusion-controlled process, but was not further investigated. There is no change in the d spacings of the *M* phase over its range of occurrence and the temperature range of the *M* to *E* transition is maximum at the $KTaO_3$ composition and decreases in both directions (Fig. 5), indicating that it is the *M* polymorph of $KTaO_3$ that is responsible for this exotherm throughout its range.

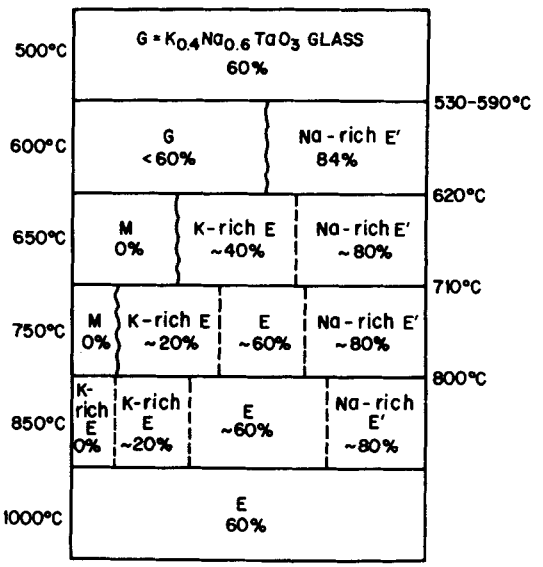

Fig. 7. Transformation of quenched $K_{0.4}Na_{0.6}TaO_3$ glass with temperature; Na content of each phase is given in percent.

The second slow reaction is found at $K_{0.8}Na_{0.2}TaO_3$ to $K_{0.4}Na_{0.6}TaO_3$. The first fraction of the stable KTaO-$NaTaO_3$ solid solution to crystallize is Na-rich compared to the composition of the glass being examined (E' in Fig. 5 and Table I). When the temperature exceeded the completion point of the *M* to *E* transformation, the diffraction peaks were rather broad, indicating a mixture containing several solid solution compositions. The diffraction peaks reached the shape and position corresponding to the starting composition only near the melting point. The 20% Na-containing glass initially crystallized 50% Na-containing phase *E*, the 40% Na glass initially crystallized as 52% Na, and the 60% Na glass initially crystallized as 84% Na. Figure 7 shows the transformation sequence inferred for the composition $K_{0.4}Na_{0.6}TaO_3$.

Similar diagrams can be drawn for the other compositions in the system. The diffusion-controlled reaction within the solid solution *E* phase is so gradual that it was not detectable during DTA. Scanning electron microscopy of a sample corresponding to the 600°C stage of Fig. 7 showed the star-shaped regions of Fig. 8; the X-ray energy spectrometer showed that the light regions were higher in Na content than the dark noncrystallized glass regions. The star shape indicates growth from a central nucleus and appears to be similar to the exsolution of crystalline $NaNbO_3$ from a silica glass.[31]

This behavior is consistent with the presence of a metastable subsolidus two-glass region in the system $K_xNa_{1-x}TaO_3$, one of which is K-rich and the other Na-rich. The two glasses could coexist as formed or phase-separate coincident with initial crystallization. At $x = 0.8$ and 0.6 the two glasses crystallize simultaneously into *M* (plus perhaps some *E*) in the K-rich and into E' in the Na-rich glass. For $x = 0.4$ the Na-rich glass crystallizes first. An electron microscopy study would be needed to confirm the details of this proposed subsolidus phase separation.

Ternary compositions shown at the right of Fig. 5 and in Fig. 6 demonstrate that the *N*, *M*, and crystal-only fields extend well into the body of the ternary system.

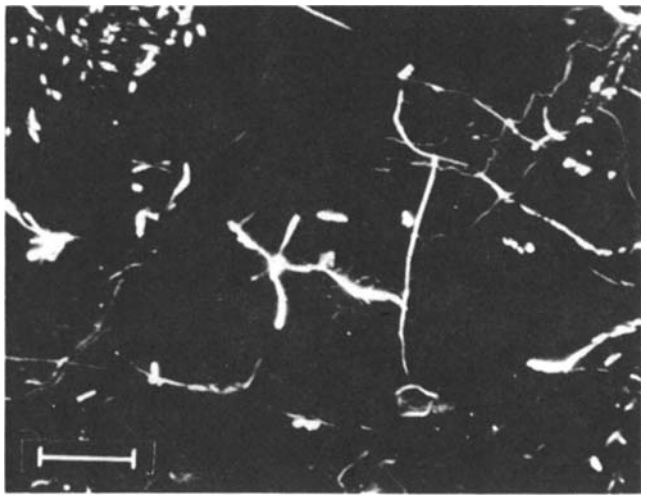

Fig. 8. Scanning electron micrograph of $K_{0.4}Na_{0.6}TaO_3$; bright areas are Na-rich (bar = 50 μm).

V. Summary

Glass was obtained by rapid quenching in most of the system $(Li,Na,K)TaO_3$. Several crystallization paths were observed on heating and two metastable crystalline phases appeared. One was a defect pyrochlore structure centered at $KTaO_3$ and the other, near $Li_{0.8}K_{0.2}TaO_3$, could not be indexed. Some transformations are rapid, whereas others are slow and diffusion-controlled. One of the slow transformations appears to involve a two-glass subsolidus region in the system $(K,Na)TaO_3$.

Acknowledgment: The writers thank R. L. Barns for use of the Guinier camera and J. W. Shiever for assistance with sample preparation.

References

[1] A. M. Glass, M. E. Lines, K. Nassau, and J. W. Shiever, "Anomalous Dielectric Behavior and Reversible Pyroelectricity in Roller-Quenched $LiNbO_3$ and $LiTaO_3$ Glass," *Appl. Phys. Lett.*, **31** [4] 249–51 (1977).

[2] A. M. Glass and K. Nassau; pp. 149–53 in Proceedings of the Conference on Rapid Solidification Processing. Edited by R. Mehrabian. Washington, D. C., November 1977; in press.

[3] K. Nassau, C. A. Wang, and M. Grasso, "Quenched Metastable Glassy and Crystalline Phases in the Lithium-Sodium-Potassium Metatantalate Pseudo-Ternary System"; submitted to the *Journal of the American Ceramic Society*.

[4] (*a*) A. M. Glass, K. Nassau, and T. J. Negran, "Ionic Conductivity of Quenched Alkali Niobate and Tantalum Glasses," *J. Appl. Phys.*, **49** [5] 4808–11 (1978).
(*b*) A. M. Glass and K. Nassau; unpublished work.

[5] B. C. Giessen and R. H. Willens; pp. 103–41 in Phase Diagrams: Materials Science and Technology, Vol. 3. Edited by A. M. Alper. Academic Press, New York, 1970.

[6] H. Jones, "Splat Cooling and Metastable Phases," *Rep. Progr. Phys.*, **36** [11] 1425–97 (1973).

[7] H. Jones and C. Suryanarayana, "Rapid Quenching from the Melt: An Annotated Bibliography 1958–72," *J. Mater. Sci.*, **8** [8] 705–53 (1973).

[8] P. T. Sarjeant and R. Roy, "New Glassy and Polymorphic Oxide Phases Using Rapid Quenching Techniques," *J. Am. Ceram. Soc.*, **50** [10] 500–503 (1967).

[9] T. Suzuki and A. M. Anthony, "Rapid Quenching on the Binary Systems of High-Temperature Oxides," *Mater. Res. Bull.*, **9** [6] 745–53 (1974).

[10] J. Coutures, F. Sibieude, and M. Foex, "Study at High Temperature of the Systems Formed by the Sesquioxides of Lanthanum with the Sesquioxides of the Lanthanides: II," *J. Solid State Chem.*, **17** [4] 377–84 (1976).

[11] J. Coutures, G. Benezech, and M. E. Antic, "Refractory Glasses Based on Alumina and Neodymium Sesquioxide," *Mater. Res. Bull.*, **10**, 539–46 (1975).

[12] T. Kokubo, M. Nishimura, and M. Tashiro, "Glass Formation in the Systems (K or Cs)$_2$O-(Nb or Ta)$_2$O$_5$-Al$_2$O$_3$," *J. Non-Cryst. Solids*, **15** [2] 329–38 (1974).

[13] T. Kokubo, S. Ito, and M. Tashiro, "Formation of Metastable Pyrochlore-Type Crystals in Glasses," *Bull. Inst. Chem. Res., Kyoto Univ.*, **51** [5] 315–28 (1973).

[14] S. Ito, T. Kokubo, and M. Tashiro, "Formation of a Metastable Pyrochlore-Type Crystal in K(Ta,Nb)O$_3$-Containing Glasses and Its Relation to Structure of the Glasses," *Yogyo Kyokai Shi*, **81** [8] 327–33 (1973).

[15] P. T. Sarjeant and R. Roy; pp. 725–33 in Reactivity of Solids. Edited by J. W. Mitchell, R. C. DeVries, R. W. Roberts, and P. Cannon. Wiley & Sons, New York, 1969.

[16] R. G. Gossink, 'Properties of Vitreous and Molten Alkali Molybdates and Tungstates," *Phillips Res. Rep., Suppl.*, **1971**, No. 3, pp. 1–106.

[17] H. S. Chen and C. E. Miller, "Rapid Quenching Technique for the Preparation of Thin Uniform Films of Amorphous Solids," *Rev. Sci. Instrum.*, **41** [8] 1237–38 (1970).

[18] J. W. Visser, "A Fully Automated Program for Finding the Unit Cell from Powder Data," *J. Appl. Crystallogr.*, **2** [3] 89–95 (1969).

[19] R. Roy; pp. 51–60 in Advances in Nucleation and Crystallization in Glasses. Edited by L. L. Hench and S. W. Freiman. American Ceramic Society, Columbus, Ohio, 1971.

[20] D. E. Day, "Mixed Alkali Glasses—Their Properties and Uses," *J. Non-Cryst. Solids*, **21** [3] 343–72 (1976).

[21] Powder Diffraction File. Joint Committee on Powder Diffraction Standards, Swarthmore, Pa.

[22] Landolt-Boernstein Numerical Data and Functional Relationships in Science and Technology, New Series, Group 3: Crystal and Solid State Physics, Vol. 3 (1969) and Vol. 9 (1975). Edited by K. H. Hellwege. Springer-Verlag, New York.

[23] T. G. Davis, "Soft Phonon Modes in the Mixed Crystal Systems $K_xNa_{1-x}TaO_3$ and $KTa_xNb_{1-x}O_3$," *J. Phys. Soc. Jpn.*, **28** [Suppl.] 245–48 (1970).

[24] D. G. Demurov, Yu. N. Venevtsev, and G. S. Zhdanov, "X-Ray Analysis and Study of the Dielectric Properties of Solid Solutions Based on the Ferroelectric $KTaO_3$," *Sov. Phys.-Crystallogr.*, **16** [2] 297–300 (1971).

[25] B. C. Giessen; pp. 227–81 in Developments in the Structural Chemistry of the Alloy Phases. Edited by B. C. Giessen. Plenum, New York, 1969.

[26] A. F. Wells, Structural Inorganic Chemistry, 4th ed; pp. 209, 439. Clarendon, Oxford, England, 1975.

[27] R. W. G. Wyckoff, Crystal Structures, Vol. 4, 2d ed.; p. 439ff. Wiley-Interscience, New York, 1968.

[28] Quoted in M. Volmer, Kinetics of Phase Formations; p. 7. I. Steinkopff, Dresden, Federal Republic of Germany, 1939.

[29] T. P. Seward III; pp. 295–338 in Phase Diagrams: Materials Science and Technology, Vol. 1. Edited by A. M. Alper. Academic Press, New York, 1970.

[30] R. Roy; pp. 13–27 in Phase Transitions, 1973. Edited by H. K. Henisch, R. Roy, and L. E. Cross. Pergamon, New York, 1973.

[31] M. M. Layton and A. Herczog, "Nucleation and Crystallization of $NaNbO_3$ from Glasses in the Na_2O-Nb_2O_3-Nb_2O_5-SiO_2 System," *J. Am. Ceram. Soc.*, **50** [7] 369–75 (1967).

Effect of MoO_3 Addition on the Grain Growth Kinetics of a Manganese Zinc Ferrite

G. C. JAIN, B. K. DAS, and N. C. GOEL*

Division of Materials, National Physical Laboratory, New Delhi–110 012 India

The effect of MoO_3 addition on the grain growth and densification kinetics of a high permeability manganese zinc ferrite was studied. Grain growth in the presence of a small amount of MoO_3 occurs in two main stages characterized by a faster rate of grain growth accompanied by rapid densification and pore coalescence in the first stage, when the MoO_3 is present as a liquid phase along the grain boundaries, and comparatively slower rates of grain growth and densification than those for the basic composition in the second stage, when MoO_3 evaporates from the matrix. The activation energies for grain growth in these stages suggested that surface and volume diffusion mechanisms were operating in the first and second stages respectively.

Received March 25, 1977; revised copy received November 15, 1977.

Based in part on a thesis submitted by N. C. Goel for the Ph. D. degree in physics, University of Delhi, Delhi, India, May 1977.

Supported in part by financial aid provided by the Council for Scientific and Industrial Research, India, to N. C. Goel.

*Now with the R & D Center for Iron and Steel, Steel Authority of India, Ltd., RANCHI–834002 (Bihar) India.